Abdominal Imaging

Published online: 6 June 2012

Abdom Imaging (2013) 38:511–526
DOI: 10.1007/s00261-012-9918-y

Rare hepatic malignant tumors: dynamic CT, MRI, and clinicopathologic features: with analysis of 54 cases and review of the literature

Yan Tan, En-hua Xiao

Department of Radiology, Second Xiangya Hospital, Central South University, Changsha 410011, Hunan, China

Abstract

Aim: To evaluate the dynamic CT, MRI, and clinicopathologic characteristics of rare hepatic malignant tumors (HRMTs), improving the understanding and diagnosis of the tumors.
Methods: A retrospective analysis of 54 cases of HRMTs diagnosed by pathology in our hospital during January 1, 2005 to September 1, 2011.
Results: The types of tumors included hepatic sarcoma ($n = 8$), malignant lymphoma ($n = 4$), malignant fibrous histiocytoma (MFH, $n = 7$), malignant melanoma (MM, $n = 4$), squamous cell carcinoma (SCC, $n = 5$), primary clear cell carcinoma of the liver (PCCCL, $n = 7$), stromal tumors (ST $n = 4$), hepatoblastoma (HB, $n = 8$), carcinoid ($n = 6$), primary primitive neuroectodermal tumor (pPNET, $n = 1$). Age of the patients ranged from 1 to 79 years (mean = 46.7 years). There were more men in this group (34/54). Symptoms of HRMTs show no specificity. Except PCCCL and HB, the serum AFP of most HRMTs was negative. 43 patients had a single hepatic mass, and 11 patients had multiple hepatic masses. Diameters ranged from 2 to 15 cm (mean = 7.7 cm). Precontrast CT revealed that most masses had uneven density ($n = 46$) and ill-demarcated margin ($n = 37$). Enhanced CT showed most lesions unevenly enhanced ($n = 49$), of which PCCCL had a prompt enhancement in the arterial phase and rapid wash-out on the portal venous phase and delayed phase; malignant lymphoma and ST had slight enhancement, MFH and undifferentiated embryonal sarcoma had gradual delayed enhancement. Most masses had low-signal on T1WI and high-signal on T2WI, while MM had high-signal on T1WI and low-signal on T2WI.
Conclusions: Although there is frequent overlap in the CT, MRI, and clinicopathologic appearances between the rare malignant tumors, some HRMTs have characteristic imaging features that can suggest a specific diagnosis.

Key words: Hepatic—Rare malignant tumors—CT—MRI—Clinicopathology

Malignancy of the liver includes neoplastic lesions that either originate in the liver or are metastatic from other tissues. Except for hepatocellular carcinoma and cholangiocarcinoma, other types of malignant tumors are quite rare [1]; it may be clinically, radiologically and morphologically difficult to correctly diagnosis.

It presents a clinical dilemma, as they are not only unusual but also often asymptomatic until they become large, and even they have nonspecific symptoms. Most patients do not have evidence of hepatitis or cirrhosis and are negative in alpha-fetoprotein (AFP) [1–3]. Survival rates of rare hepatic malignant tumors (HRMTs) remain discouraging. Although there is frequent overlap in the CT, MRI, and clinicopathologic appearances between the rare malignant tumors, some HRMTs have characteristic imaging features that can suggest a specific diagnosis. Herein, we present 54 cases of HRMTs which were proven by pathology and review of the literature.

Materials and methods

Clinical data

We have collected 54 cases of HRMTs diagnosed by pathology from 2708 cases of hepatic malignant tumors (HMT) during January 1, 2005 to September 1, 2011 in our hospital. Every patient underwent dynamic CT examination (8 patients had CT examination in other hospitals), of which 15 patients underwent dynamic MRI examination before operation. 40 patients

Correspondence to: En-hua Xiao; *email:* cjr.xiaoenhua@vip.163.com

underwent tumor resection, while 14 patients underwent biopsy. Our Institutional Review Board (IRB) approved this retrospective study, and informed consent was waived.

Equipment and methods

Using SIEMENS SOMATOM Sensation 64 CT. Scan parameters were as follows: layer thickness: 3 mm; layer from: 5 mm, vision field: 25 × 25–38 × 38 cm^2, matrix: 512 × 512. Using Iohexol as CT contrast agent, dose: 1.5 mL/kg, injection flow rate: 2.5 mL/s. Hepatic arterial phase (HAP) scanning began about 25–30 s after injection, hepatic venous phase (HVP) scanning began at 50 s, and hepatic delayed phase (HDP) scanning began at 5 min. Adopting PHILIPS 3.0T superconducting MRI. Scan parameters were as follows: body coil, thickness: 6 mm, layer from: 1.5 mm, vision field: 380 × 380, matrix: 288 × 288; using respiratory-triggered fast spin-echo (FFE) T1WI sequence: TR 10 ms, TE 2.3 ms; respiratory triggered fast spin-echo T2 fat suppression (TSET2) sequence: TR 2000 ms, TE 70 ms; FFET1-enhanced sequence. Using Gd-DTPA as MRI contrast agent, dose: 0.2 mg/kg, injection flow rate: 1.5 mL/s. HAP scanning began about 25–30 s after injection, HVP scanning began at 50 s, and HDP scanning began at 5 min. All the original films were reviewed by two readers specialized in gastrointestinal imaging.

Results

Clinical findings (Table 1)

Age of the patients ranged from 1 to 79 years (mean = 46.7 years). There were more men in this group (34/54). 33 cases presented with right upper abdominal quadrant intermittent pain or discomfort, 10 were incidentally found to have a mass of the liver in physical examination, fever (n = 1), skin stained yellow sclera (n = 2), left shoulder pain (n = 1), fatigue and anorexia (n = 3), diarrhea and melena (n = 3), dysphagia (n = 1). Except for primary clear cell carcinoma and hepatoblastoma, the serum AFP levels of most tumors remained within the normal range. 13 patients had a history of hepatitis B virus infection. The postoperative follow-up rate was 64.85% (35/54), and the overall survival time was 11 months.

Pathological findings

The types of tumors included hepatic sarcoma (n = 8, carcinosarcoma 2, leiomyosarcoma 2; angiosarcoma 2; undifferentiated embryonal sarcoma 1; fibrosarcoma 1), malignant lymphoma (n = 4), malignant fibrous histiocytoma (MFH, n = 7), malignant melanoma (MM, n = 4), squamous cell carcinoma (SCC, n = 5), primary clear cell carcinoma of the liver (PCCCL, n = 7),

Table 1. The clinical findings of HRMTs

Tumor types	Cases	Proportion of HMT	Mean age (years)	Sex (M/F)	Hepatitis B virus infection	AFP (+)	Treatment	Overall survival (months)
Sarcoma	8	0.29%	55.5	5/3	0	0	Hepatectomy 7 TACE 1	5
Malignant lymphoma	4	0.15%	54.3	4/0	1	0	Hepatectomy 2 TACE 2	13
MFH	7	0.25%	44	4/3	2	1	Hepatectomy 6 TACE 1	15
MM	4	0.15%	38.3	3/1	0	0	Hepatectomy 2 TACE 1	8
SCC	5	0.18%	56.8	2/3	0	0	Hepatectomy 2 TACE 2 RFA 1	5
PCCCL	7	0.25%	54.4	5/2	7	6	Hepatectomy 6 TACE 1	12
ST	4	0.15%	49	1/3	1	0	Hepatectomy 3 RFA 1	19
HB	8	0.29%	17.6	5/3	0	7	Hepatectomy 5 TACE 2 LT 1	20
Carcinoid	6	0.22%	51.4	5/1	2	1	Hepatectomy 3 TACE 3	7
pPNET	1	0.03%	66	0/1	0	0	Hepatectomy	4
Total	54	2.2%	46.7	34/20	13/54	15/54	–	11

HRMTs hepatic rare malignant tumors, *HMT* hepatic malignant tumors (2708 cases), *MFH* malignant fibrous histiocytosarcoma, *MM* malignant melanoma, *SCC* squamous cell carcinoma, *PCCCL* primary clear cell carcinoma of the liver, *ST* stromal tumors, *HB* hepatoblastoma, *AFP* alpha-fetoprotein, *RFA* radiofrequency ablation, *LT* liver transplantation. Overall survival time: the time during from finding lesions to death. pPNET: peripheral primary primitive neuroectodermal tumor.

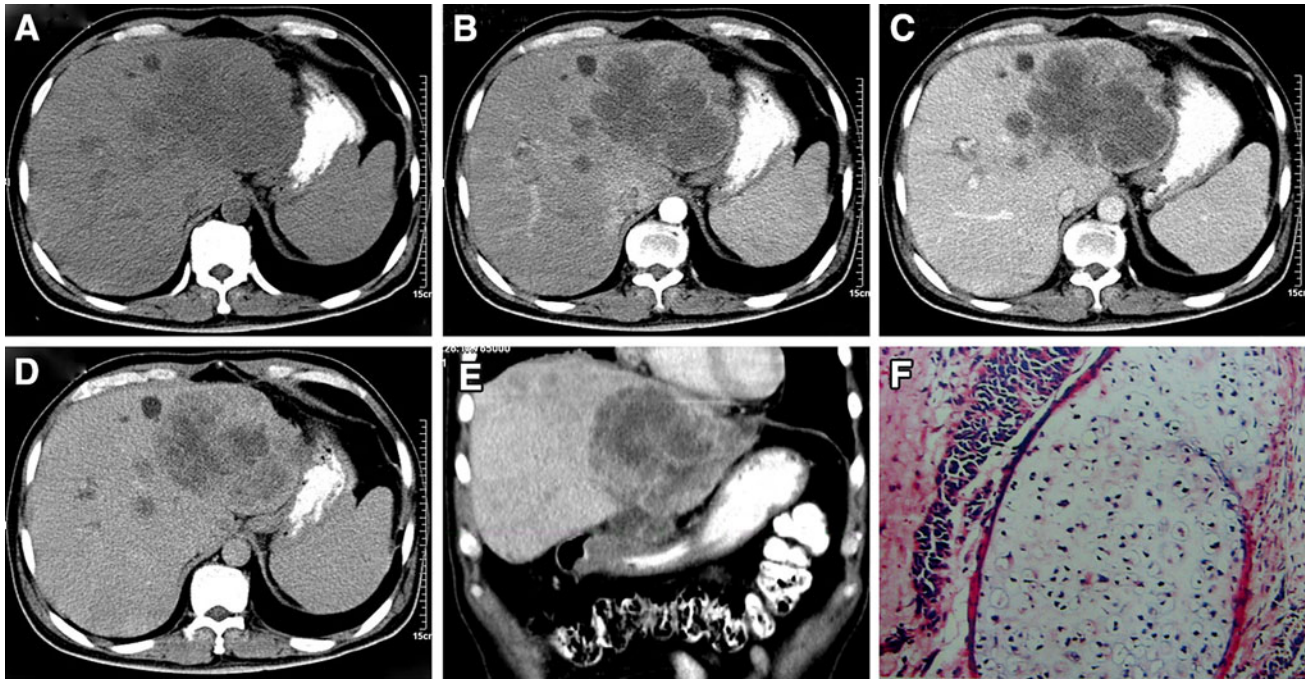

Fig. 1. Carcinosarcoma in a 56-year-old man. Precontrast CT scan shows a lobular low-density mass with well-defined border and satellite lesions in left lobe of the liver (**A**), enhanced CT scan demonstrates the mass heterogeneously enhanced on arterial phase (HAP) (**B**) and on portal venous phase (PVP) (**C**), and most areas of tumors become isodensity with normal liver on delayed phase (HDP) (**D**), coronal reconstruction of the portal venous phase (**E**). HE staining (**F**, ×200): tumor tissue contains carcinomatous and sarcomatous ingredients, and the immature cartilage can be seen.

stromal tumors (ST $n = 4$), hepatoblastoma (HB, $n = 8$), carcinoid ($n = 6$), primary primitive neuroectodermal tumor (pPNET, $n = 1$). MM, SCC, ST, and carcinoid contained primary tumor and metastasis tumor from other sites. The cases of metastasis tumors of MM, SCC, ST, and carcinoid were 3, 3, 2, and 4, respectively.

Dynamic CT, MRI findings

43 patients had a single hepatic mass [right lobe ($n = 30$), left lobe ($n = 11$), caudate lobe ($n = 2$)], and 11 patients had multiple masses. Precontrast CT scan revealed that most masses had uneven density ($n = 46$) with necrosis or hemorrhage, and ill-demarcated margin ($n = 37$). Diameters ranged from 2 to 15 cm (mean = 7.7 cm). Enhanced CT showed most lesions unevenly enhanced ($n = 49$), of which the PCCCL had a prompt enhancement on HAP and rapid wash-out on PVP and HDP, the malignant lymphoma and ST had slight enhancement, and the MFH and undifferentiated embryonal sarcoma had gradually delayed enhancement (Figs. 1, 2, 3, 4, 5, 6, 7, 8, 9, 10, 11, 12; Table 2).

Most masses had low-signal on T1WI image and high-signal on T2WI image, while malignant melanoma (MM) was hyperintense on T1-weighted images and hypointense on T2-weighted images. The enhancement was the same with the CT scan. Most patients ($n = 41$) had no signs of hepatitis and cirrhosis, and most masses did not violate the portal vein and bile duct system ($n = 39$).

Discussion

Primary hepatic sarcoma

Primary hepatic sarcoma is a rare entity. It represents <1% of all malignant hepatic tumors [4]. In our group, the proportion of primary hepatic sarcoma was 0.29%. There were eight cases of hepatic sarcomas, consisting of two cases of carcinosarcomas, two leiomyosarcomas, two angiosarcomas, one undifferentiated sarcoma, and one fibrosarcoma. None of them had history of hepatitis B virus infection, and AFP levels remained within the normal range.

Primary hepatic carcinosarcoma (PHCS) is a rare malignant hepatic tumor [5]. It contains both carcinomatous and sarcomatous ingredients [6]. It occurs most commonly in men aged 50–70 years and indicates a poor prognosis due to highly invasive and metastatic features [7]. CT and MRI findings of PHCS may show a large, irregular, lobulated, and low-attenuation mass with necrotic or cystic area [7].

Primary hepatic leiomyosarcoma (PHLS) originates from smooth muscle cells of the hepatic veins or bile duct [8]. The tumor commonly occurs in middle-age or older patients with equal-sex distribution [9]. Grossly, PHLS usually presents as a single large mass [10]. CT findings of PHLS have been described as a large, well-defined, heterogeneous-hypodensity mass with internal and peripheral enhancement [9, 11] or cystic mass with an enhancing thick wall [8, 10].

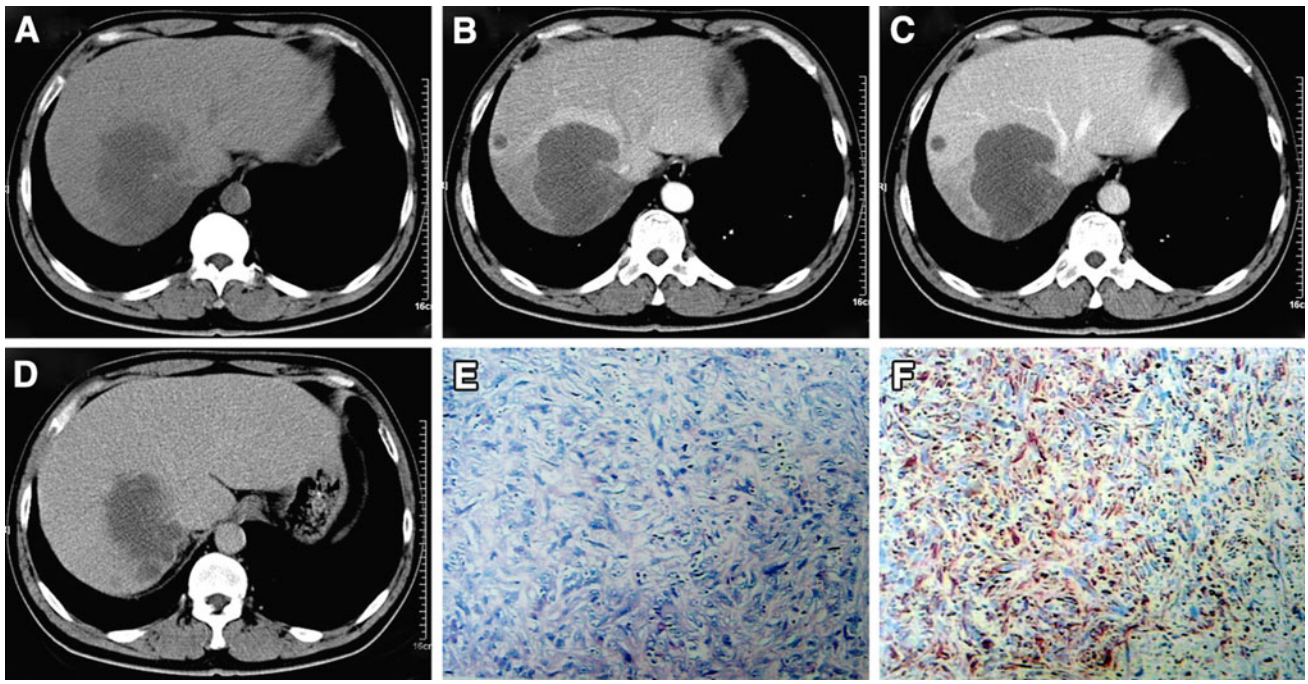

Fig. 2. Fibrosarcoma in a 42-year-old man. Precontrast CT scan shows a lobular low-density mass with necrosis and ill-defined border in the right lobe of the liver (**A**), enhanced CT scan demonstrates the mass has rim enhanced on HAP (**B**) and on PVP (**C**), and peripheral areas of tumors become isodensity with normal liver on HDP (**D**), HE staining (**E**, ×100): tumor cells are fat and spindle shaped. Immunohistochemical staining (**F**, ×100): *brown* particles in cytoplasm and nucleus are on behalf of Vim positive.

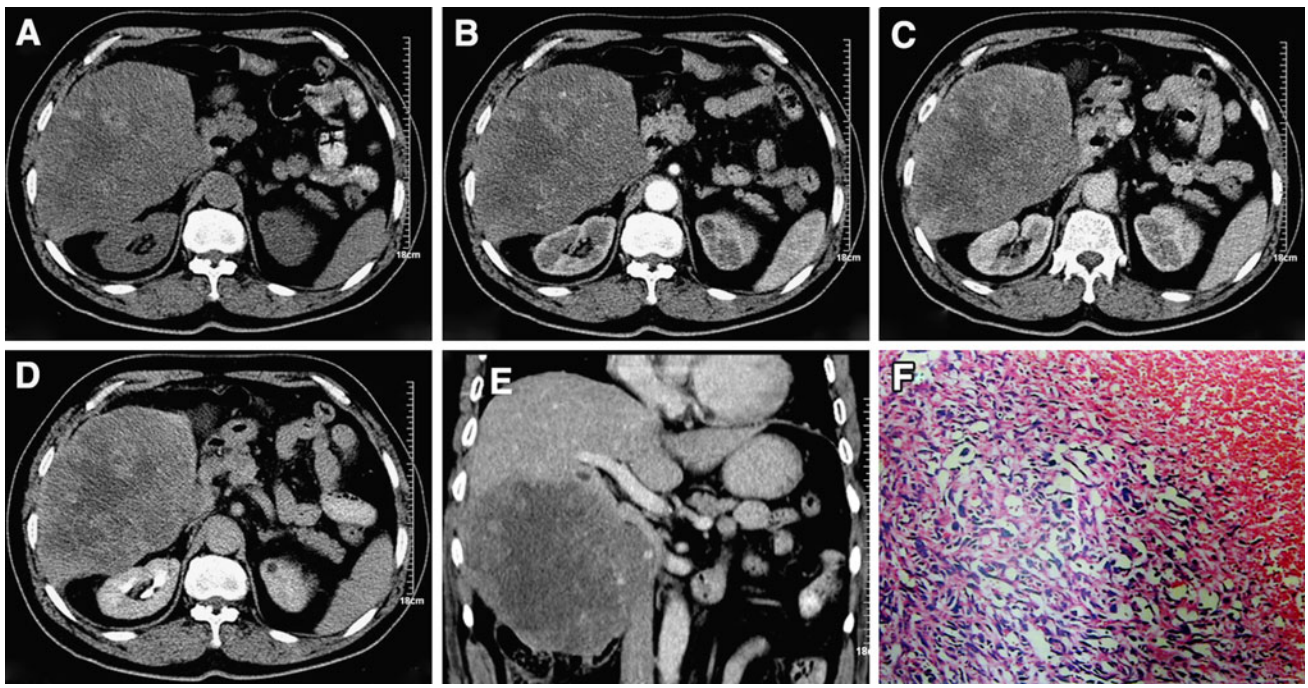

Fig. 3. Angiosarcoma in a 72-year-old man. Precontrast CT scan reveals a heterogeneous low-density mass with hemorrhage in the right lobe of the liver (**A**), enhanced CT scan shows the mass slightly and heterogeneously enhanced on HAP (**B**) and PVP (**C**), and delayed enhancement (**D**), coronal reconstruction of the PVP (**E**). HE staining (**F**, ×100): This section of tumor demonstrates tightly packed, slit-like vascular channels lined by spindle-shaped endothelial cells. The cells have eosinophilic cytoplasm, and large nuclei.

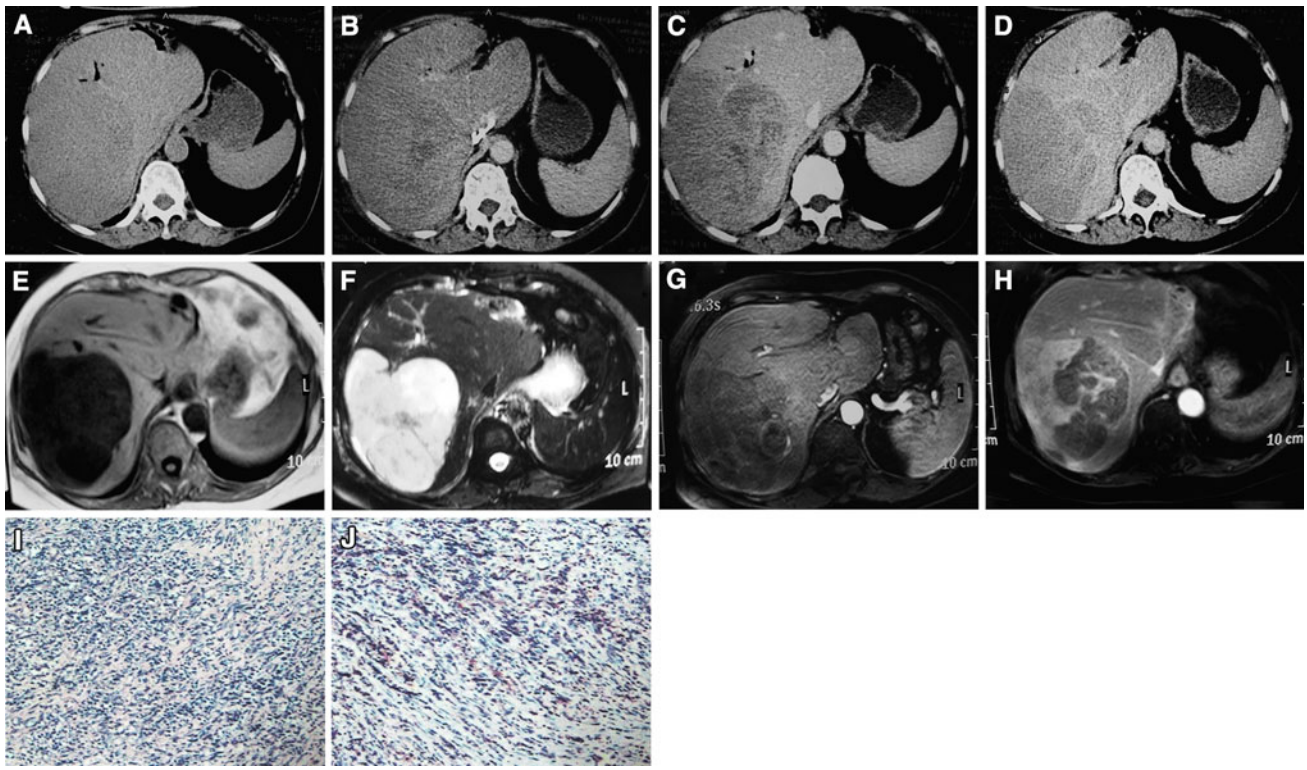

Fig. 4. Lymphoma in a 25-year-old man. Precontrast CT scan shows a large low-density mass with demarcated margin in the right lobe of the liver (**A**), enhanced CT scan demonstrates the mass slightly and heterogeneously enhanced on HAP (**B**) and PVP (**C**), and delayed enhancement (**D**), precontrast MRI scan shows the mass as hypointense on T1WI (**E**) and hyperintense on T2WI (**F**), and heterogeneous enhancement (**G** and **H**). HE staining (**I**, ×100) shows the diffuse distribution of small round tumor cell. Immunohistochemical staining (**J**, ×100): *brown* particles in cytoplasm and nucleus are on behalf of leukocyte common antigen (LCA) positive.

Primary hepatic angiosarcoma (PHAS) accounts for only 2% of primary hepatic tumors. It most commonly occurs in men between 50 and 70 years of age and has a poor prognosis [4, 12]. A male predominance has been reported [13]. PHAS accounts for only 0.07% of primary hepatic malignant tumors in our group. The gross appearance of PHAS evaluated by pathology shows four types of growth patterns: a large dominant mass, multiple nodules, mixed patterns of a dominant mass with nodules, and a diffusely infiltrating micronodular tumor [12, 14]. PHAS has various appearances at CT or MR imaging which reflects varied histologic composition. When PHAS appears as a massive lesion, MR images show hemorrhagic and heterogeneous appearance. Studies suggest that differentiation of PHAS from other malignant neoplasms by MRI is difficult; especially because the number of cases is limited [15].

Undifferentiated embryonal sarcoma (UES) of the liver was first described as a clinicopathological entity in 1978 [16]. The tumor has a very slight male predominance [17]. UES is a solid lesion with central necrosis or hemorrhage. The CT findings typically appear as a large, predominantly cystic mass with well-defined border and delayed enhancement [18], as in our case. On MRI imaging, the tumor has low-signal on T1WI and high-signal on T2WI. The tumor shows a peripheral enhancement of a surrounding pseudocapsule on early enhanced MR, and may show enhancement of tumor nodules on HDP. Metastases may be seen in lung and bone, brain and skin [19].

The CT findings of primary hepatic sarcoma in our group are similar to the literature. The masses were more common in right lobe (6/8). Diameters ranged from 5 to 15 cm (mean = 9.7 cm). Precontrast CT scan revealed that masses were with uneven density and ill-demarcated margin. Contrast-enhanced CT showed the lesions unevenly enhanced.

Malignant lymphoma

Hepatic primary lymphoma constitutes about only 0.016% of nonHodgkin's lymphoma (NHL) [20]. The patients commonly present with right upper abdominal quadrant discomfort or fever. Hepatic primary lymphoma is easily identified on CT scans, whereas secondary lymphoma is often diffusely infiltrate and difficult to detect [21]. There are three morphologic patterns in hepatic lymphoma: large solitary masses

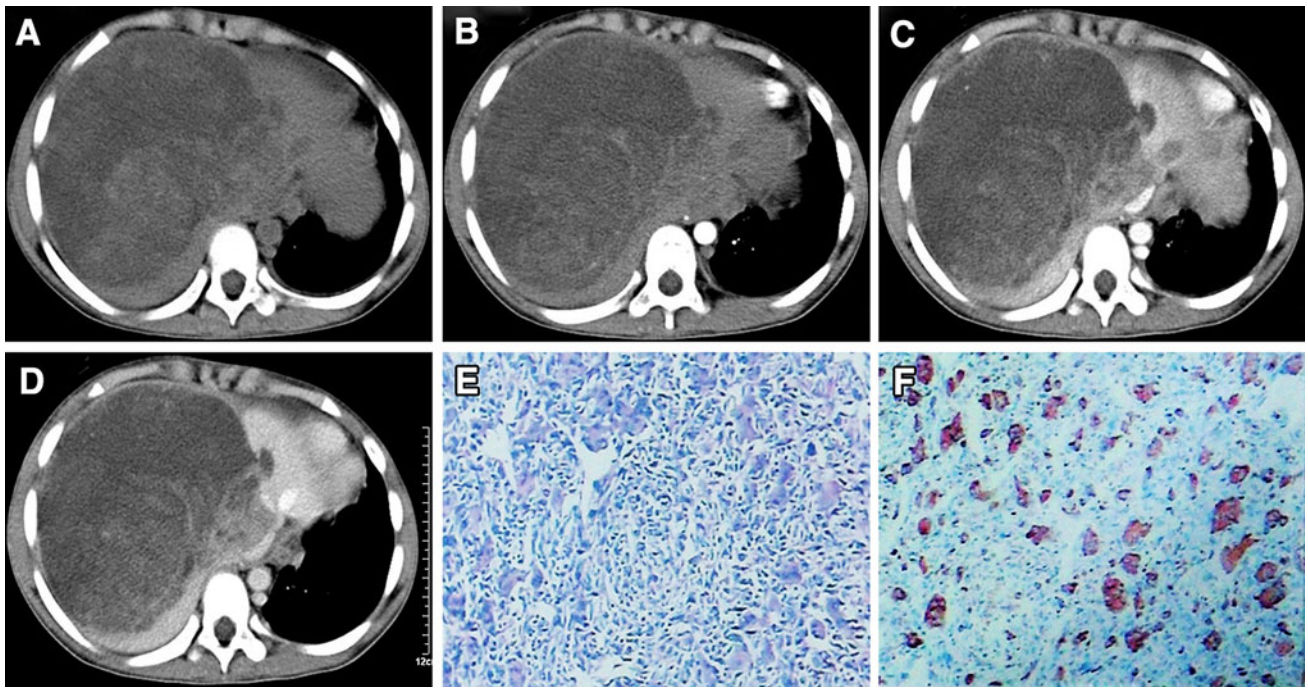

Fig. 5. Malignant fibrous histiocytosarcoma in a 10-year-old female child. Precontrast CT scan shows a large, heterogeneous low-density mass in the right lobe of the liver with well-defined border (**A**), enhanced CT scan shows the cystic wall and fibrous septa enhanced on HAP (**B**) and on PVP (**C**), and better enhancement on HDP (**D**). HE staining (**E**, ×200,) identifies that the tumor is well demarcated with surrounding liver parenchyma and consists of spindle cells and histiocyte-like cells. Immunohistochemical staining (**F**, ×200): *brown* particles in cytoplasm and nucleus are on behalf of vimentin positive.

(>4 cm), multiple focal nodules, and diffuse infiltrative type. There are two cases of primary lymphoma and two cases of secondary lymphoma in our group, and diffusely infiltrative hepatic lymphoma was not observed.

Hepatic lymphoma appears as low-density lesions on unenhanced and contrast-enhanced CT scans, or has a thin enhancing rim [22, 23]. The CT characteristics of hepatic secondary lymphoma include blood vessel floating sign and enhancement [24]. MRI findings show that the lesions present hypointense on T1WI and hyperintense on T2WI. MRI can distinguish diffuse infiltration from normal liver tissue in cases in which neither sonography nor CT demonstrates any abnormalities [25]. MRI can be used in NHL patients with a clinical suspicion of hepatic involvement when sonography and CT do not show any focal lesions. Positron emission tomography (PET) using deoxyglucose (FDG) scan has been performed for further evaluation [26]. FDG–PET/CT showed diffuse intense FDG uptake in the enlarged liver and spleen, with systemic FDG-avid lymphadenopathy including the hepatic hilar nodes [27]. However, none of the imaging findings is specific for hepatic lymphoma.

The CT findings of hepatic lymphoma in our group are similar to the literature. Precontrast CT and MRI scan revealed that the masses were with even density (3/4) and well-demarcated margin (4/4). Contrast-enhanced CT showed the lesions slightly enhanced. The hepatic secondary lymphoma in our group also presented with large solitary masses, not the diffusely infiltrative type. We recommend that in a large mass with even density and slight enhancement the possibility of lymphoma should be considered.

Malignant fibrous histiocytosarcoma

Malignant fibrous histiocytosarcoma (MFH) is the most common soft tissue sarcoma in adults, usually involving the deep fascia, extremities, or retroperitoneum [28]. Originating in the liver is very unusual. It has five histological subtypes: storiform pleomorphic, giant cells, myxoid, inflammatory, and angiomatoid [29]. Hepatic MFH usually occurs in men between 50 and 60 years of age. The 2-year survival rate is approximately 60%, and 20% suffers from local recurrence [30]. We had even cases of hepatic MFH, the mean age was 44 years, there was a slight male predominance (4/7), and the mean survival time was 15 months.

CT findings of hepatic MFH include: large, heterogeneously enhancing mass with necrotic areas, single enhancing peripheral pseudocapsule mass or cystic mass with cystic wall and fibrous septa enhancement [29, 31–33]. Better enhancement of the solid component and fibrous septa may be seen on delayed CT scan [29].

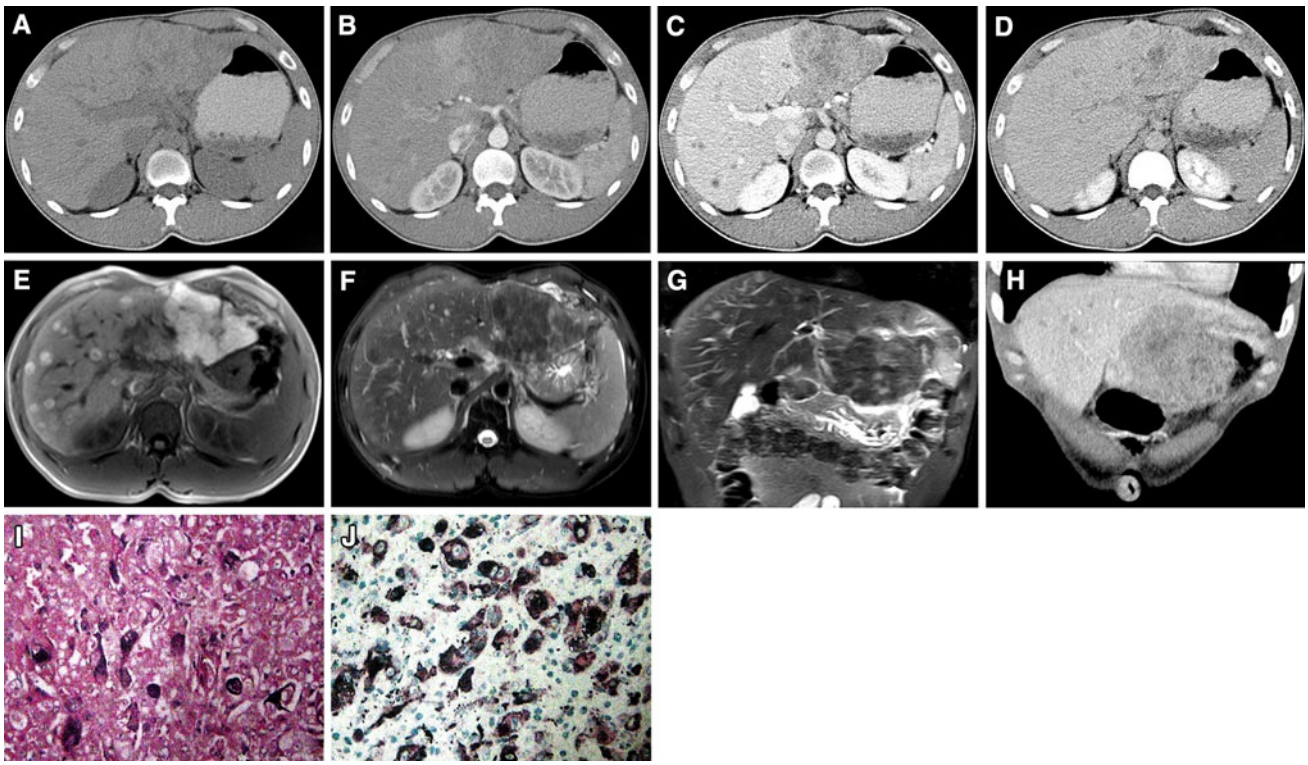

Fig. 6. Malignant melanoma in a 25-year-old woman. Precontrast CT scan shows an isoattenuation mass with ill-defined margin in the left lobe of the liver (**A**), enhanced CT scan shows the mass slightly and heterogeneously enhanced (**B**–**D**); MRI scan demonstrates multiple lesions in the liver, hyperintense on T1WI (**E**) and hypointense on T2WI (**F**), coronal reconstruction of MRI and CT (**G**, **H**). HE staining (**I**, ×200): the tumor cells disclose obvious atypia, with abundant cytoplasm and large nucleus. Immunohistochemical staining (**J**, ×200): *brown* particles in cytoplasm and nucleus are on behalf of HMB45 positive.

There is no evidence of portal vein invasion, bile duct obstruction, or lymph node metastasis [29]. MRI findings show the mass is with low-signal on T1WI and high-signal on T2WI. Enhanced MRI findings were the same with CT scan [29]. The imaging findings of MFH in our group were in accord with the literature. Precontrast CT and MRI scan revealed that the masses were with heterogeneous density (7/7) and ill-demarcated margin (5/7). Contrast-enhanced CT showed solid component and septa had delayed enhancement.

Hepatectomy, systemic chemotherapy, or trans-arterial chemoembolization (TACE) could be considered for the treatment.

Malignant melanoma

Malignant melanoma (MM) is an aggressive tumor with a tendency to metastasize. Hepatic metastasis of MM is not unusual and may occur after a clinically long latent period [34]. The primary MM is really rare. There are four cases of malignant melanoma of which one was primary MM and three were metastases in our group. The prognosis of patients with MM liver metastases is very poor; the 1-year survival is estimated at 10% [35] and occurs in about 14%–20% of patients in clinical series [36]. The mean survival time of MM in our group was 8 months. F-18 FDG–PET has been proposed as the standard imaging modality for staging high-risk patients [37, 38]. MRI has also proven to be sensitive in the detection of liver metastases compared to other imaging modalities such as CT [39] and PET [40]. It appears that MRI detects metastases a few months earlier than PET scan. Precontrast MR images appear sufficient to screen for liver metastases in patients with MM [40, 41].

Precontrast CT showed that the mass was a huge, solid hyperintense lesion with central necrosis or hemorrhage. Calcifications could be seen in the solid components. Contrast CT showed that the solid component had slight enhancement [42–45]. MRI imaging can provide more useful information than CT, and shows the characteristic features of hyperintense on T1WI and hypointense on T2WI [39]. The same findings were evident in our group. The mean diameter was 7.8 cm. Precontrast CT scan revealed that the masses were with slight hyperdensity (3/4) and ill-demarcated margin (4/4), some mass had necrotic areas, and there were no visible calcifications. Contrast-enhanced CT showed the lesions unevenly enhanced. Precontrast MRI showed the characteristic features, and found more lesions than CT scan.

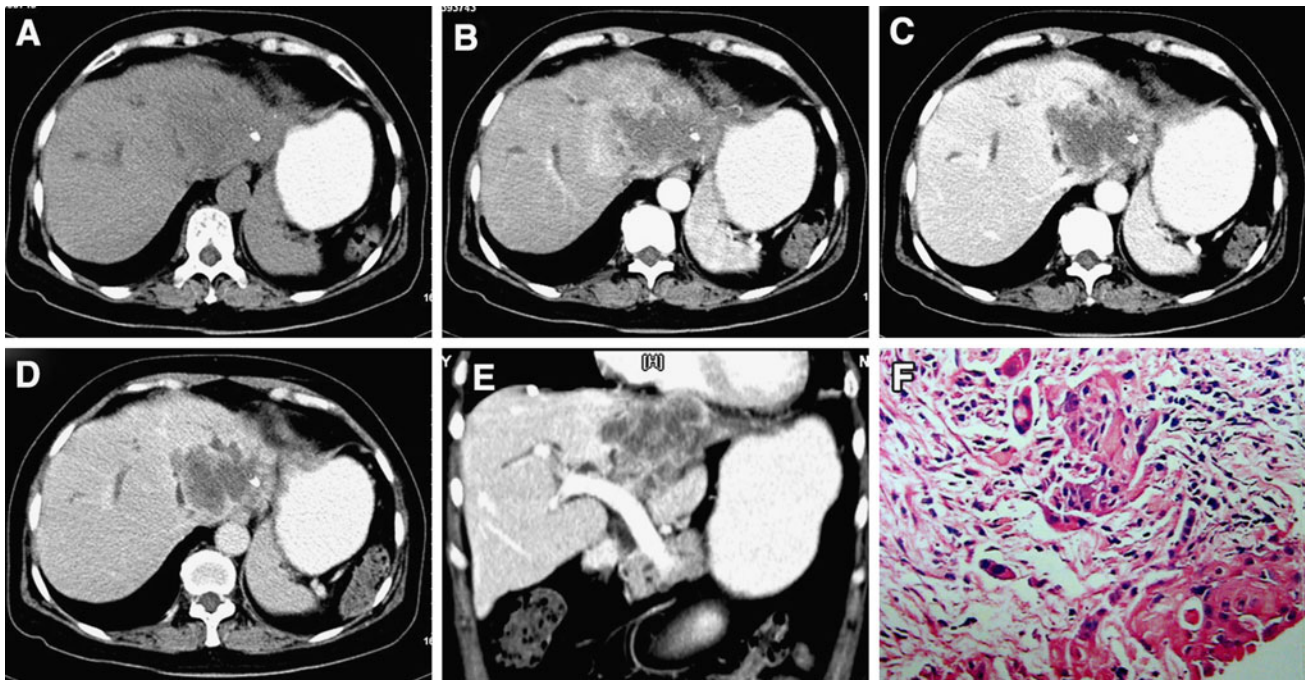

Fig. 7. Squamous cell carcinoma in a 65-year-old woman. Precontrast CT scan shows an irregular low-density mass in the left lobe of the liver with ill-defined border (**A**), with small pieces of calcification. Enhanced CT scan shows the mass has irregular ring enhancement on HAP (**B**) and PVP (**C**), and has concentric delayed enhancement (**D**). HE staining (**F**, ×200) shows the tumor tissue consists of pleomorphic cells with marked intercellular bridges and focal keratinization.

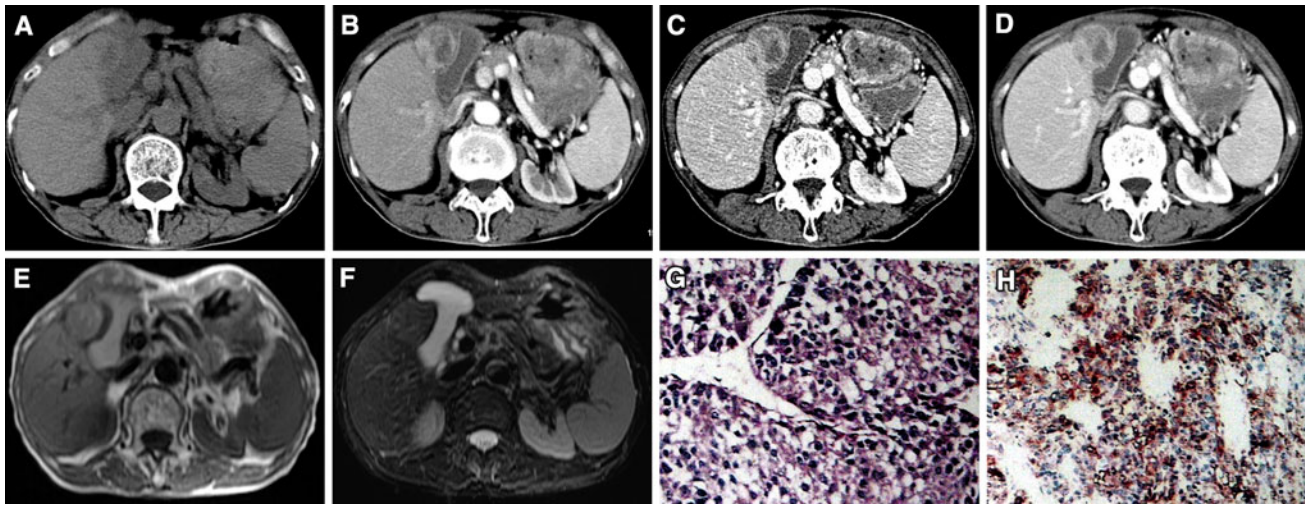

Fig. 8. Primary clear cell carcinoma in a 70-year-old man. Precontrast CT scan shows a heterogeneous low-density nodule in the left lobe of the liver (**A**), enhanced CT scan demonstrates the nodule has irregular ring enhancement on HAP (**B**) and PVP (**C**), with delayed enhancement (**D**), MRI scan shows the nodule has isoattenuation on T1WI (**E**) and T2WI (**F**). HE staining (**G**, ×200) discloses the mass is mainly composed of clear cells, with clear cell boundaries and clear membrane. Immunohistochemical staining (**H**, ×200): *brown* particles in cytoplasm and nucleus are on behalf of AFP positive.

Criteria such as plasmacytoid morphology, spindled cells, melanin-like pigment, and necrosis were helpful in the diagnosis of MM. Immunoperoxidase staining showed the expected staining pattern of positivity for HMB-45 and S-100 protein [46]. Despite conventional surgery for resectable segmental or lobar liver involvement, systemic chemotherapy, chemoimmunotherapy, or proton beam irradiation, the median survival of patients with liver metastases is <6 months [47]. TACE can be considered to be a safe treatment for liver metastases of uveal malignant melanoma offering a symptomatic or even palliative treatment option [41].

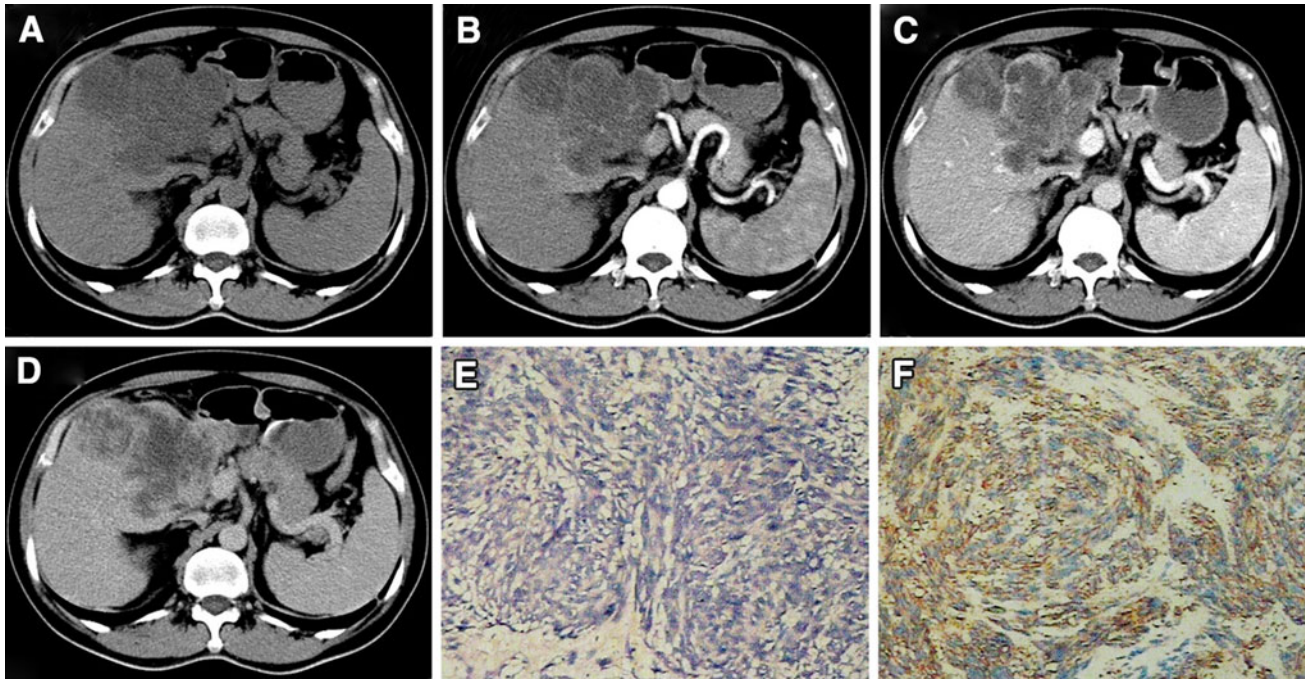

Fig. 9. Stromal tumor in a 53-year-old man. Precontrast CT scan reveals an irregular low-density mass with demarcated margin in the left lobe of the liver (**A**), enhanced CT scan shows the mass has slight irregular ring enhancement (**B**–**D**). HE staining (**E**, ×100) discloses neoplastic spindle cells in an irregular pattern. Immunohistochemical staining (**F**, ×100): *brown* particles in cytoplasm and nucleus are on behalf of CD117 positive.

Squamous cell carcinoma

Hepatic primary squamous cell carcinoma (SCC) is rare and reported sporadically. It has been reported to be associated with hepatic teratoma, hepatolithiasis, or hepatic cysts with chronic inflammation and metaplasia [42, 48–51]. Because of portal vein invasion and disseminated metastases, the prognosis is very poor, with no survival longer than 1 year ever having been reported [42, 52, 53]. Metastatic SCC of the liver mostly originates from nasopharyngeal cancer, cervical cancer, lung cancer, or upper esophageal cancer. In our group, there were two cases of primary SCC and three cases of metastatic SCC.

Precontrast CT showed that the lesion was a huge, predominantly cystic mass with a solid component and irregular wall. Calcifications were seen in the solid components. Contrast CT showed that the solid component and irregular wall had enhancement [42–45]. MRI showed that the mass was hypointense on T1-weighted images and hyperintense on T2-weighted images [42]. Furthermore, given the current knowledge about the origin of SCC, sonographic follow-up of hepatic cysts should be needed, and surgical resection may be recommended in the case of large cysts with unclear sonographic findings [54]. The same findings were evident in our group. Precontrast CT scan revealed that the masses were with uneven hypodensity (5/5) and ill-demarcated margin (4/5), and with small pieces of calcification. Contrast-enhanced CT showed the lesions unevenly enhanced.

Microscopically, the tumor tissues consist of variable-sized solid tumor nests with middle- to large-sized cells with intercellular bridge formation and focal keratinization [42]. Hepatectomy, systemic chemotherapy (5-fluorouracil and cisplatin), or TACE could be considered for the treatment [55, 56].

Primary clear cell carcinoma

Primary clear cell carcinoma of the liver (PCCCL) is a rare subtype of primary hepatocellular carcinoma (HCC). The clinical characteristics of the PCCCL are similar to those of conventional HCC. The frequency is between 2.2% and 6.7% among HCC reported in the literature [57, 58]. Lai et al. [59] suggested that the diagnosis of hepatic CCC could be made even when the proportion of clear cells was $<30\%$, while Buchanan et al. [60] suggested that PCCCL should be diagnosed when the proportion of clear cells was $>30\%$. However, tumors with clear cells ranging from 90% to 100% are extremely rare [61]. Most studies are diagnosed PCCCL when the proportion of clear cells was $>50\%$ [58, 62, 63]. The rates of hepatitis B virus infection and capsule formation were higher in PCCCL patients than in those with HCC. However, no remarkable differences in

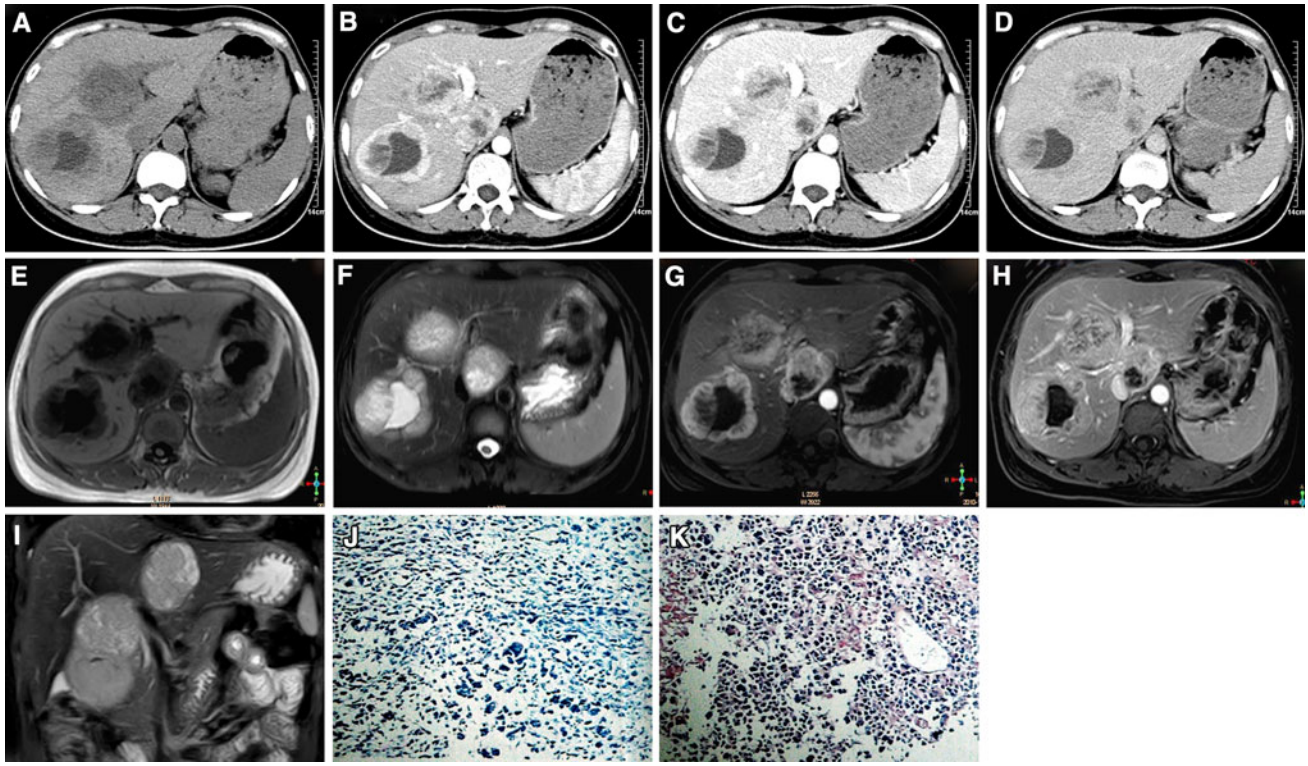

Fig. 10. Hepatoblastoma in a 65-year-old woman. Precontrast CT scan shows three low-density masses with necrosis and demarcated margin in the liver (**A**), enhanced CT scan shows the masses significantly enhanced on HAP (**B**) and PVP (**C**), and with isoattenuation on HDP (**D**), precontrast MRI scan demonstrates the masses are hypointense on T1WI (**E**) and hyperintense on T2WI (**F**), on enhanced MRI the masses have significantly and heterogeneously enhancement (**G**, **H**). HE staining (**I** ×100, **J** ×200) discloses tumor cells have obvious atypia, and tumor cells are arranged in adenoid or acinar-like shape.

patients' sex, age, AFP-positive rate or the location, size, number, and grade of tumors were observed between the two groups [57]. Both the tumor types were prone to occur in patients with hepatitis B virus infection and liver cirrhosis [57]. There are seven cases of PCCCL in our group; the serum AFP levels of most tumors (6/7) were high. All the patients had history of hepatitis B virus infection.

Pseudocapsule formation is an important gross pathologic feature of HCC. Pseudocapsule indicates a relatively positive prognosis after tumor resection [64]. The pseudocapsule presents as rim enhancement, and MRI is more sensitive than CT in identifying the finding [64–66]. Because of hypervascular blood supply, typical HCC shows early enhancement at HAP, and rapid washout at PVP or HDP [67, 68]. The imaging characteristics of PCCCL are similar to those of HCC [69]. These imaging features may help differentiate PCCCL from other liver tumors. The CT and MRI findings of our patients were the same as mentioned above, but one patient had delayed enhancement.

Surgical resection is an effective way to achieve favorable outcomes and even long-term survival of the patients with hepatic PCCCL [58, 70]. Ji showed that the prognosis was related to the proportion of clear cells. The greater the number of clear cells, the better the prognosis. Postoperative chemotherapy with calcium folinate and tegafur had no obvious effect on survival time of patients [63].

Stromal tumors

Stromal tumor (ST) is seen mostly in the gastrointestinal tract and predominantly occurs in the stomach (60%–70%) and small intestine (25%–35%), with rare occurrences in the colon and rectum (5%), esophagus (<2%) and appendix [71, 72]. Liver metastasis is the most predominant site, accounting for about 50% of all the cases. There have been only few reports of hepatic primary ST so far [73, 74]. Lymph node metastases are rare. The postoperative 5-year survival rate was 30%, with a median survival of 39 months [75]. There were two cases of hepatic primary ST and two cases of metastatic ST in our group, the mean age was 49 years and mean survival time was 19 months.

Imaging features of ST have an exophytic and cavitary nature with heterogeneous enhancement [76, 77]. In Vanel's report [76], 13 cases of hepatic metastases from

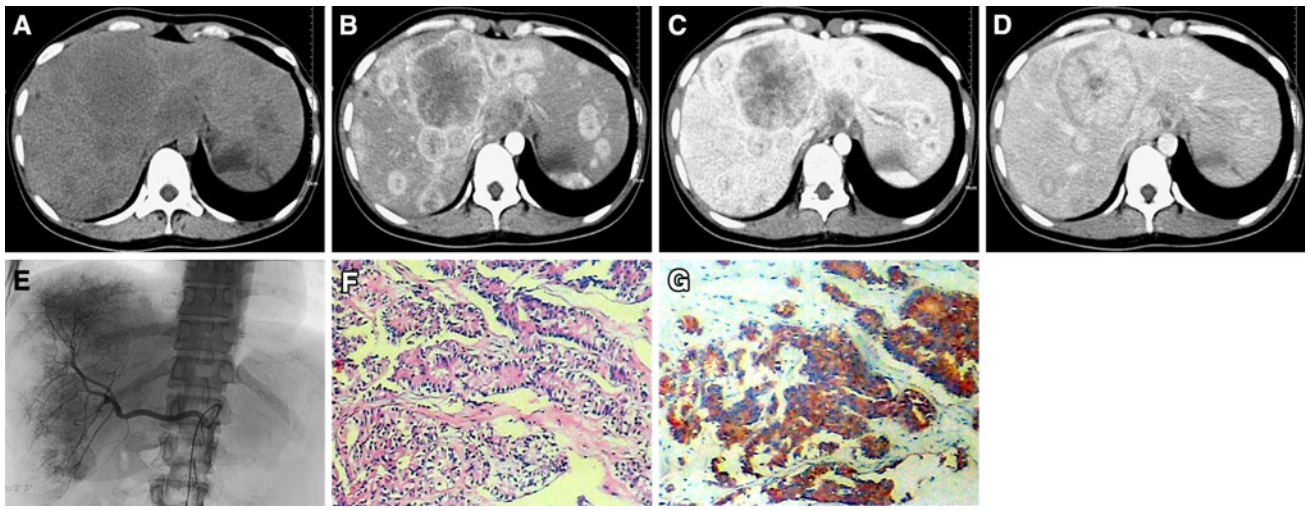

Fig. 11. Carcinoid in a 25-year-old woman. Precontrast CT scan shows multiple low-density masses with ill-defined border in the liver (**A**), on enhanced CT scan, the masses are significantly enhanced on HAP (**B**) and PVP (**C**), and the enhancement decreases on HDP (**D**), angiography (**E**) demonstrates the masses have rich blood supply. HE staining (**F**, ×100) discloses islands of cells are separated by vascularized septa. The cells are discohesive with small nucleoli, powdery chromatin, and no observable cytoplasm. Immunohistochemical staining (**G**, ×100): *brown* particles in cytoplasm and nucleus are on behalf of Syn positive.

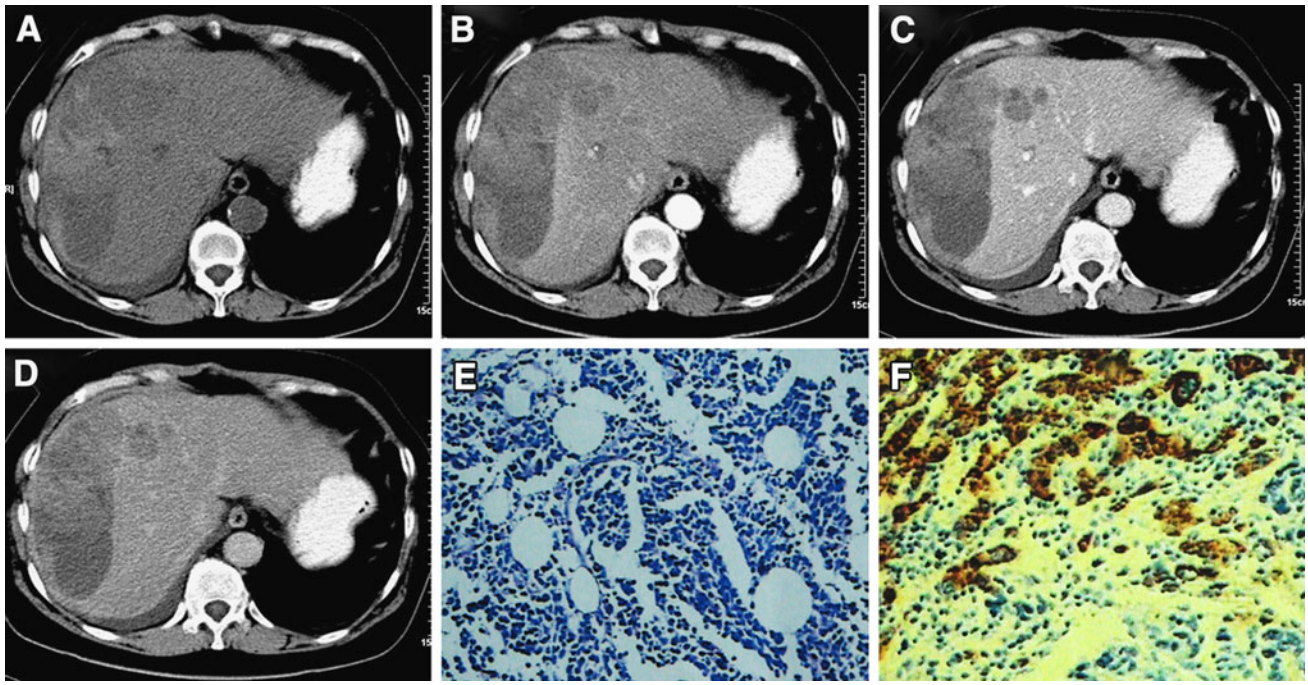

Fig. 12. Peripheral primary primitive neuroectodermal tumor in a 66-year-old woman. Precontrast CT scan shows an irregular low-density mass with hemorrhage and ill-defined margin in the right lobe of the liver (**A**), on enhanced CT scan, the mass has slight ring enhancement (**B**–**D**). HE staining (**E**, ×100) discloses the small round cells distributed like flake or nest. Immunohistochemical staining (**F**, ×100): *brown* particles in cytoplasm and nucleus are on behalf of CD99 positive.

gastrointestinal ST were heterogeneous hypodense lesions with progressive, concentric enhancement. The masses of ST in our group were with heterogeneous density and ill-defined borders, and had slight heterogeneous enhancement.

Surgery is the preferred management for ST where feasible. Localized resection with a clear margin of 1–2 cm seems to be adequate treatment [78]. Imatinib mesylate, a tyrosine kinase inhibitor, is an effective treatment for locally advanced unresectable static ST,

Table 2. The dynamic CT and MRI findings of HRMTs

Tumor types	Cases	Location	Mean size (cm)	Density (uneven)	Border (ill-defined)	Enhancement
Sarcoma	8	Right lobe 6 left lobe 2	9.7	8	4	7
Malignant lymphoma	4	Right lobe 2 left lobe 1 caudate lobe 1	8.9	2	2	3
MFH	7	Right lobe 5 left lobe 1	9.1	6	5	7
MM	4	Right lobe 2 multiple masses 2	7.8	3	3	4
SCC	5	Right lobe 1 left lobe 1 multiple masses 3	6.1	5	4	5
PCCCL	7	Right lobe 6 left lobe 1	6.4	7	7	7
ST	4	Right lobe 2 left lobe 2	7.5	3	3	3
HB	8	Right lobe 4 left lobe 1 caudate lobe 1 multiple masses 3	9.5	7	4	8
Carcinoid	6	Right lobe 1 left lobe 2 multiple masses 3	3.2	5	5	6
pPNET	1	Right lobe	5.3	1	0	1
Total	54	–	7.7	46	37	49

HRMTs hepatic rare malignant tumors, *MFH* malignant fibrous histiocytosarcoma, *MM* malignant melanoma, *SCC* squamous cell carcinoma, *PCCCL* primary clear cell carcinoma of the liver, *ST* stromal tumors, *HB* hepatoblastoma, *pPNET* peripheral primary primitive neuroectodermal tumor.

and imatinib mesylate and transplantation are effective agents for molecularly targeted treatment [79]. Tumor size and mitotic counts are used as prognostic factors, and mitotic counts exceeding 5 per 50 high power fields or size larger than 5 cm can predict recurrence or metastasis to other areas [76, 80].

Hepatoblastoma

Hepatoblastoma (HB) has an incidence of 0.6/100000, accounting for approximately 60%–85% of all hepatic tumors in children [81, 82]. Most of the children are between 6 months and 3 years of age. Children usually present with abdominal distension, abdominal pain, or gastrointestinal disorders [83], serum AFP is typically raised in 90% of patients [81]. The AFP negative hepatic lesions can still be a malignant HB [84], which include a small cell undifferentiated component and are thought to be more aggressive [85]. We have eight cases of HB, six cases were children (mean age = 5 years), two cases were adult (mean age = 47 years), AFP levels of most patients (7/8) were raised. None of the patients had history of hepatitis B virus infection.

Macroscopically, HB consists of a large multinodular expansile mass with necrosis and hemorrhage, well demarcated but not encapsulated. Histopathological classification of HB has been divided two types: pure epithelial and mixed epithelial and mesenchymal [86].

Unenhanced CT typically shows a relatively well-defined, heterogeneous slightly hypodense mass, with or without calcifications. On contrast-enhanced CT, the tumor reveals a heterogeneous enhancement, which may be hyperdense on the early HAP and usually appears iso- or hypodense on HDP. On MR images, HB is iso- or hyperintense on T2WI and iso- or hypointense on T1WI. The enhancement of contrast MRI is similar with CT and quite nonspecific [87, 88]. The tumor has a tendency to invade hepatic and portal veins. In our group, pre-contrast CT and MRI scan revealed that the masses were with heterogeneous density (8/8) and ill-demarcated margin (5/8), three cases had calcification. Contrast-enhanced CT showed the lesions had heterogeneous enhancement.

The foundation of HB management is surgical resection [89] and preoperative chemotherapy could cause the tumor to shrink, allowing removal of a previously unresectable tumor [90, 91]. Liver transplantation for HB also has been recommended [92]. New methodologies have been applied for local control, including TACE [93] and radiofrequency ablation (RFA) [94] for advanced-stage and metastatic tumors.

Hepatic carcinoid

Carcinoid is the most common neuroendocrine tumor. It comprises 1%–2% of all gastrointestinal malignancies [95, 96]. Metastases to the liver are approximately 5%–10% of gastrointestinal carcinoid [96–98]. Hepatic primary carcinoids are very rare. We had four cases of metastatic carcinoid from the pancreases and sigmoid colon, and one case of hepatic primary carcinoid. There were no signs of carcinoid syndrome in our patients. The typical histological appearance is small uniform cells arranged in nests, cords, and trabeculae, containing both neuroendocrine and carcinoma components [99].

The radiologic characteristics of hepatic primary carcinoid have not been well defined, but the case reports reviewed show that the lesions are typically solid with necrotic components [100–105]. Earlier reports have described hepatic metastatic carcinoid lesions as solid, hypervascular masses [106, 107]. Carcinoid hepatic metastases may be difficult to identify and delineate on CT as they may be isointense on PVP imaging. A combination of precontrast, HAP, and PVP imaging will improve the sensitivity of detection [107]. Selective angiography detects 20% more liver metastases than CT [108]. In MRI series of 156 metastatic lesions, using multi-phase enhanced scans, 94% were hypervascular, and 6% were hypovascular. None were primarily cystic

[109]. Kuker suggested delayed phase FDG–PET/CT improves lesion detectability in primary and metastatic liver disease, revealing new lesions in 17% of the patients [110]. Most patients (4/5) of our group had multiple masses. The CT and MRI findings had no specificity, so it was difficult to diagnose correctly before operation.

Primary primitive neuroectodermal tumor

Primitive neuroectodermal tumor (PNET) is a rare malignant tumor originating from neuroectoderm and consists of primitive undifferentiated small round cells [111]. The term PNET was coined by Hart and Earle in 1973 [112]. It can be classified into two types: Central-type (cPNET) and peripheral-type (pPNET) [111]. The majority of PNETs occur in the central nervous system (CNS) of children [113, 114]. Peripheral PNET often occurs in the thoracopulmonary region (Askin tumor), retroperitoneum, and extremities [115]. Involvement of visceral organs by PNET is particularly rare. Involvement of the liver has been reported in the form of metastasis from other primary sources [116, 117]. There are only a few cases of primary hepatic neuroectodermal tumor reported worldwide in the literature [118, 119].

In pPNET patients, the tumors often demonstrated ill-defined, large soft tissue masses (>5 cm on average) and exhibited aggressive spread to the normal tissue. Calcification and lymphadenopathy are uncommon at presentation [120–122]. The tumor often demonstrated isodensity with necrotic areas on precontrast CT images, or isointensity or hypointensity on T1-weighted MR images and heterogeneous hyperintensity on T2-weighted MR images. On contrast-enhanced CT/T1WI, the tumor showed heterogeneous enhancement [123, 124]. In our group, the tumor demonstrated heterogeneous hyperintensity mass with necrosis and hemorrhage within it, and had slight heterogeneous ring enhancement.

Histopathology of the PNET revealed that these tumors had poorly differentiated small round cell morphology. Immunohistochemistry revealed CD-99-positive [125]. The therapeutic protocol of PNET is similar to that used for Ewing's sarcoma because of similarities between the two tumors [126, 127]. The focus of pPNET therapy incorporates surgery, chemotherapy, and radiation therapy. Yao showed that early Chromogranin A (CgA) and neuron-specific enolase (NSE) responses were potential prognostic markers for treatment in patients with advanced PNET [128]. pPNET can progress rapidly, and metastasis and local extensions are often found during initial diagnosis [127, 129]. The overall survival rate of pPNET is poor and with 5-year disease-free survival rate of 45%–55% [130]. The patient in our group died of lung metastasis about 3 months after operation.

Conclusion

Some HRMTs have characteristic imaging features that can suggest a specific diagnosis, although there is frequent overlap in the CT, MRI, and clinical appearances of HRMTs. Our study showed that excepting PCCCL and HB, the serum AFP levels of most HRMTs remained within normal range. PCCCL had prompt enhancement on HAP and rapid wash-out on PVP and HDP; lymphoma and ST had slight enhancement, and the MFH and undifferentiated embryonal sarcoma had gradually delayed enhancement. Other types of rare hepatic tumors generally had heterogeneous enhancement.

Acknowledgments. This work was supported by The National Natural Science Foundation of China, Nos 30070235, 30470508, and 30870695; The Natural Science Foundation of Hunan Province, Nos 06JJ2008 and 07JJ6040.

References

1. Perilongo G, Shafford EA (1999) Liver tumours. Eur J Cancer 35(953–958):958–959
2. Finn JP, Hall-Craggs MA, Dicks-Mireaux C, et al. (1990) Primary malignant liver tumors in childhood: assessment of resectability with high-field MR and comparison with CT. Pediatr Radiol 21:34–38. doi:10.1007/BF02010811
3. Rasalkar DD, Chu WC, Cheng FW, et al. (2010) A pictorial review of imaging of abdominal tumours in adolescence. Pediatr Radiol 40(1552–1561):1589–1590. doi:10.1007/s00247-010-1738-z
4. Weitz J, Klimstra DS, Cymes K, et al. (2007) Management of primary liver sarcomas. Cancer 109:1391–1396. doi:10.1002/cncr.22530
5. Wang XW, Liang P, Li HY (2004) Primary hepatic carcinosarcoma: a case report. Chin Med J (Engl) 117:1586–1587
6. Kwon JH, Kang YN, Kang KJ (2007) Carcinosarcoma of the liver: a case report. Korean J Radiol 8:343–347. doi:10.3348/kjr.2007.8.4.343
7. Lao XM, Chen DY, Zhang YQ, et al. (2007) Primary carcinosarcoma of the liver: clinicopathologic features of 5 cases and a review of the literature. Am J Surg Pathol 31:817–826. doi:10.1097/01.pas.0000213431.07116.e0
8. Ferrozzi F, Bova D, Zangrandi A, et al. (1996) Primary liver leiomyosarcoma: CT appearance. Abdom Imaging 21:157–160. doi:10.1007/s002619900034
9. Gates LK, Cameron AJ, Nagorney DM, et al. (1995) Primary leiomyosarcoma of the liver mimicking liver abscess. Am J Gastroenterol 90:649–652
10. Soyer P, Bluemke DA, Riopel M, et al. (1995) Hepatic leiomyosarcomas: CT features with pathologic correlation. Eur J Radiol 19:177–182. doi:10.1016/0720-048X(94)00592-Z
11. Fujita H, Kiriyama M, Kawamura T, et al. (2002) Primary hepatic leiomyosarcoma in a woman after renal transplantation: report of a case. Surg Today 32:446–449. doi:10.1007/s005950200073
12. Koyama T, Fletcher JG, Johnson CD, et al. (2002) Primary hepatic angiosarcoma: findings at CT and MR imaging. Radiology 222:667–673. doi:10.1148/radiol.2223010877
13. Locker GY, Doroshow JH, Zwelling LA, et al. (1979) The clinical features of hepatic angiosarcoma: a report of four cases and a review of the English literature. Medicine (Baltimore) 58:48–64
14. Kojiro M, Nakashima T, Ito Y, et al. (1985) Thorium dioxide-related angiosarcoma of the liver. Pathomorphologic study of 29 autopsy cases. Arch Pathol Lab Med 109:853–857
15. Ohtomo K, Araki T, Itai Y, et al. (1992) MR imaging of malignant mesenchymal tumors of the liver. Gastrointest Radiol 17:58–62. doi:10.1007/BF01888510
16. Stocker JT, Ishak KG (1978) Undifferentiated (embryonal) sarcoma of the liver: report of 31 cases. Cancer 42:336–348. doi:10.1002/1097-0142(197807

17. Buetow PC, Buck JL, Pantongrag-Brown L, et al. (1997) Undifferentiated (embryonal) sarcoma of the liver: pathologic basis of imaging findings in 28 cases. Radiology 203:779–783
18. O'Sullivan MJ, Swanson PE, Knoll J, et al. (2001) Undifferentiated embryonal sarcoma with unusual features arising within mesenchymal hamartoma of the liver: report of a case and review of the literature. Pediatr Dev Pathol 4:482–489. doi:10.1007/s10024001-0047-9
19. Boechat MI, Kangarloo H (1989) MR imaging of the abdomen in children. AJR Am J Roentgenol 152:1245–1250
20. Noronha V, Shafi NQ, Obando JA, et al. (2005) Primary non-Hodgkin's lymphoma of the liver. Crit Rev Oncol Hematol 53:199–207. doi:10.1016/j.critrevonc.2004.10.010
21. Sanders LM, Botet JF, Straus DJ, et al. (1989) CT of primary lymphoma of the liver. AJR Am J Roentgenol 152:973–976
22. Radin DR, Esplin JA, Levine AM, et al. (1993) AIDS-related non-Hodgkin's lymphoma: abdominal CT findings in 112 patients. AJR Am J Roentgenol 160:1133–1139
23. Townsend RR (1991) CT of AIDS-related lymphoma. AJR Am J Roentgenol 156:969–974
24. Wang GX, Guo DJ, Zhao JN (2010) CT image of liver secondary lymphoma. Zhonghua Gan Zang Bing Za Zhi 18:371–373. doi:10.3760/cma.j.issn.1007-3418.2010.05.014
25. Gazelle GS, Lee MJ, Hahn PF, et al. (1994) US, CT, and MRI of primary and secondary liver lymphoma. J Comput Assist Tomogr 18:412–415
26. Cheng G, Servaes S, Chamroonrat W, et al. (2010) Non-Hodgkin's lymphoma of the bone and the liver without lymphadenopathy revealed on FDG–PET/CT. Clin Imaging 34:476–479. doi:10.1016/j.clinimag.2009.11.013
27. Suga K, Kawakami Y, Hiyama A, et al. (2010) F-18 FDG PET/CT findings in a case of T-cell lymphoma-associated hemophagocytic syndrome with liver involvement. Clin Nucl Med 35:116–120. doi:10.1097/RLU.0b013e3181c7bf20
28. Weiss SW, Enzinger FM (1978) Malignant fibrous histiocytoma: an analysis of 200 cases. Cancer 41:2250–2266. doi:10.1002/1097-0142(197806)41:6<2250::AID-CNCR2820410626>3.0.CO;2-W
29. Yu JS, Kim KW, Kim CS, et al. (1999) Primary malignant fibrous histiocytoma of the liver: imaging features of five surgically confirmed cases. Abdom Imaging 24:386–391. doi:10.1007/s002619900520
30. Ding GH, Wu MC, Yang JH, et al. (2006) Primary hepatic malignant fibrous histiocytoma mimicking cystadenocarcinoma: a case report. Hepatobiliary Pancreat Dis Int 5:620–623
31. Anagnostopoulos G, Sakorafas GH, Grigoriadis K, et al. (2005) Malignant fibrous histiocytoma of the liver: a case report and review of the literature. Mt Sinai J Med 72:50–52
32. Ferrozzi F, Bova D (1998) Hepatic malignant fibrous histiocytoma: CT findings. Clin Radiol 53:699–701
33. Wunderbaldinger P, Schima W, Harisinghani M, et al. (1998) Primary malignant fibrous histiocytoma of the liver: CT and MR findings. AJR Am J Roentgenol 171:900–901
34. Satyamoorthy K, Herlyn M (2002) Cellular and molecular biology of human melanoma. Cancer Biol Ther 1:14–17
35. Bedikian AY, Legha SS, Mavligit G, et al. (1995) Treatment of uveal melanoma metastatic to the liver: a review of the M. D. Anderson Cancer Center experience and prognostic factors. Cancer 76:1665–1670. doi:10.1002/1097-0142(19951101)76:9<1665::AIDCNCR2820760925>3.0.CO;2-J
36. Rigel DS, Friedman RJ, Kopf AW (1996) The incidence of malignant melanoma in the United States: issues as we approach the 21st century. J Am Acad Dermatol 34:839–847
37. Damian DL, Fulham MJ, Thompson E, et al. (1996) Positron emission tomography in the detection and management of metastatic melanoma. Melanoma Res 6:325–329
38. Eigtved A, Andersson AP, Dahlstrom K, et al. (2000) Use of fluorine-18 fluorodeoxyglucose positron emission tomography in the detection of silent metastases from malignant melanoma. Eur J Nucl Med 27:70–75. doi:10.1007/PL00006666
39. Sica GT, Ji H, Ros PR (2000) CT and MR imaging of hepatic metastases. AJR Am J Roentgenol 174:691–698
40. Ghanem N, Altehoefer C, Hogerle S, et al. (2005) Detectability of liver metastases in malignant melanoma: prospective comparison of magnetic resonance imaging and positron emission tomography. Eur J Radiol 54:264–270. doi:10.1016/j.ejrad.2004.07.005
41. Vogl TJ, Schwarz W, Eichler K, et al. (2006) Hepatic intraarterial chemotherapy with gemcitabine in patients with unresectable cholangiocarcinomas and liver metastases of pancreatic cancer: a clinical study on maximum tolerable dose and treatment efficacy. J Cancer Res Clin Oncol 132:745–755. doi:10.1007/s00432-006-0138-0
42. Saito T, Harada K, Tsuneyama K, et al. (2002) Primary squamous cell carcinoma of the liver producing parathyroid hormone-related protein. J Gastroenterol 37:138–142. doi:10.1007/s005350200010
43. Yagi H, Ueda M, Kawachi S, et al. (2004) Squamous cell carcinoma of the liver originating from non-parasitic cysts after a 15 year follow-up. Eur J Gastroenterol Hepatol 16:1051–1056
44. Yuki N, Hijikata Y, Kato M, et al. (2006) Squamous cell carcinoma as a rare entity of primary liver tumor with grave prognosis. Hepatol Res 36:322–327
45. Abbas R, Willis J, Kinsella T, et al. (2008) Primary squamous cell carcinoma of the main hepatic bile duct. Can J Surg 51:E85–E86
46. Parwani AV, Chan TY, Mathew S, et al. (2004) Metastatic malignant melanoma in liver aspirate: cytomorphologic distinction from hepatocellular carcinoma. Diagn Cytopathol 30:247–250. doi:10.1002/dc.10394
47. Feldman ED, Pingpank JF, Alexander HJ (2004) Regional treatment options for patients with ocular melanoma metastatic to the liver. Ann Surg Oncol 11:290–297. doi:10.1245/ASO.2004.07.004
48. Hsieh CB, Chen CJ, Yu JC, et al. (2005) Primary squamous cell carcinoma of the liver arising from a complex liver cyst: report of a case. Surg Today 35:328–331. doi:10.1007/s00595-004-2941-z
49. Charles AR, Gupta AK, Bhatnagar V (2001) Giant congenital solitary cyst of the liver: report of a case. Surg Today 31:732–734. doi:10.1007/s005950170081
50. Pliskin A, Cualing H, Stenger RJ (1992) Primary squamous cell carcinoma originating in congenital cysts of the liver. Report of a case and review of the literature. Arch Pathol Lab Med 116:105–107
51. Furlanetto A, Dei TA (2002) Squamous cell carcinoma arising in a ciliated hepatic foregut cyst. Virchows Arch 441:296–298. doi:10.1007/s00428-002-0668-z
52. Doty JE, Tompkins RK (1989) Management of cystic disease of the liver. Surg Clin North Am 69:285–295
53. Clements D, Newman P, Etherington R, et al. (1990) Squamous carcinoma in the liver. Gut 31:1333–1334. doi:10.1136/gut.31.11.1333
54. Bondini S, Leoni S, Bolondi L (2005) Squamous cell carcinoma of the liver: metastasis or primary neoplasm. J Clin Ultrasound 33:477–478
55. Boscolo G, Jirillo A, Da PP (2005) Complete remission of poorly differentiated squamous liver carcinoma after systemic chemotherapy and surgery. A case report. Tumori 91:71–72
56. Kaji R, Sasaki N, Tateishi I, et al. (2003) A case report of primary hepatic squamous cell carcinoma that remarkably responded to low dose arterial injection of anti-cancer drugs. Kurume Med J 50:71–75
57. Liu Z, Ma W, Li H, Li Q (2008) Clinicopathological and prognostic features of primary clear cell carcinoma of the liver. Hepatol Res 38:291–299. doi:10.1111/j.1872-034X.2007.00264.x
58. Lao XM, Zhang YQ, Jin X, et al. (2006) Primary clear cell carcinoma of liver–clinicopathologic features and surgical results of 18 cases. Hepatogastroenterology 53:128–132
59. Lai CL, Wu PC, Lam KC, et al. (1979) Histologic prognostic indicators in hepatocellular carcinoma. Cancer 44:1677–1683. doi:10.1002/1097-0142(197911)44:5<1677::AIDCNCR2820440522>3.0.CO;2-D
60. Buchanan TJ, Huvos AG (1974) Clear-cell carcinoma of the liver. A clinicopathologic study of 13 patients. Am J Clin Pathol 61:529–539
61. Yang SH, Watanabe J, Nakashima O, et al. (1996) Clinicopathologic study on clear cell hepatocellular carcinoma. Pathol Int 46:503–509. doi:10.1111/j.1440-1827.1996.tb03645.x
62. Chung YE, Park MS, Park YN, et al. (2009) Hepatocellular carcinoma variants: radiologic-pathologic correlation. AJR Am J Roentgenol 193:W7–W13. doi:10.2214/AJR.07.3947

63. Ji SP, Li Q, Dong H (2010) Therapy and prognostic features of primary clear cell carcinoma of the liver. World J Gastroenterol 16:764–769. doi:10.3748/wjg.v16.i6.764
64. Ishigami K, Yoshimitsu K, Nishihara Y, et al. (2009) Hepatocellular carcinoma with a pseudocapsule on gadolinium-enhanced MR images: correlation with histopathologic findings. Radiology 250:435–443. doi:10.1148/radiol.2501071702
65. Grazioli L, Olivetti L, Fugazzola C, et al. (1999) The pseudocapsule in hepatocellular carcinoma: correlation between dynamic MR imaging and pathology. Eur Radiol 9:62–67. doi:10.1007/s003300050629
66. Ebara M, Ohto M, Watanabe Y, et al. (1986) Diagnosis of small hepatocellular carcinoma: correlation of MR imaging and tumor histologic studies. Radiology 159:371–377
67. Willatt JM, Hussain HK, Adusumilli S, Marrero JA (2008) MR Imaging of hepatocellular carcinoma in the cirrhotic liver: challenges and controversies. Radiology 247:311–330. doi:10.1148/radiol.2472061331
68. Jeong YY, Yim NY, Kang HK (2005) Hepatocellular carcinoma in the cirrhotic liver with helical CT and MRI: imaging spectrum and pitfalls of cirrhosis-related nodules. AJR Am J Roentgenol 185:1024–1032. doi:10.2214/AJR.04.1096
69. Liu QY, Li HG, Gao M, et al. (2011) Primary clear cell carcinoma in the liver: CT and MRI findings. World J Gastroenterol 17:946–952. doi:10.3748/wjg.v17.i7.946
70. Ye XP, Li LQ, Peng T, et al. (2010) Diagnosis and treatment of primary clear cell carcinoma of the liver. Zhonghua Zhong Liu Za Zhi 32:64–66
71. Kindblom LG, Remotti HE, Aldenborg F, et al. (1998) Gastrointestinal pacemaker cell tumor (GIPACT): gastrointestinal stromal tumors show phenotypic characteristics of the interstitial cells of Cajal. Am J Pathol 152:1259–1269
72. Miettinen M, Lasota J (2006) Gastrointestinal stromal tumors: review on morphology, molecular pathology, prognosis, and differential diagnosis. Arch Pathol Lab Med 130:1466–1478
73. Hu X, Forster J, Damjanov I (2003) Primary malignant gastrointestinal stromal tumor of the liver. Arch Pathol Lab Med 127:1606–1608
74. De Chiara A, De Rosa V, Lastoria S, et al. (2006) Primary gastrointestinal stromal tumor of the liver with lung metastases successfully treated with STI-571 (imatinib mesylate). Front Biosci 11:498–501
75. DeMatteo RP, Shah A, Fong Y, et al. (2001) Results of hepatic resection for sarcoma metastatic to liver. Ann Surg 234(540–547):547–548
76. Vanel D, Albiter M, Shapeero L, et al. (2005) Role of computed tomography in the follow-up of hepatic and peritoneal metastases of GIST under imatinib mesylate treatment: a prospective study of 54 patients. Eur J Radiol 54:118–123. doi:10.1016/j.ejrad.2005.01.012
77. Luo XL, Liu D, Yang JJ, et al. (2009) Primary gastrointestinal stromal tumor of the liver: a case report. World J Gastroenterol 15:3704–3707. doi:10.3748/wjg.15.3704
78. DeMatteo RP, Lewis JJ, Leung D, et al. (2000) Two hundred gastrointestinal stromal tumors: recurrence patterns and prognostic factors for survival. Ann Surg 231:51–58
79. Demetri GD, von Mehren M, Blanke CD, et al. (2002) Efficacy and safety of imatinib mesylate in advanced gastrointestinal stromal tumors. N Engl J Med 347:472–480
80. Miettinen M, Majidi M, Lasota J (2002) Pathology and diagnostic criteria of gastrointestinal stromal tumors (GISTs): a review. Eur J Cancer 38(Suppl 5):S39–S51
81. Litten JB, Tomlinson GE (2008) Liver tumors in children. Oncologist 13:812–820. doi:10.1634/theoncologist.2008-0011
82. Fiaschetti V, Fiori R, Gaspari E, et al. (2010) Mixed hepatoblastoma in a young male adult: a case report and literature review. Case Report Med 2010:919457. doi:10.1155/2010/919457
83. Schnater JM, Kohler SE, Lamers WH, et al. (2003) Where do we stand with hepatoblastoma? A review. Cancer 98:668–678. doi:10.1002/cncr.11585
84. Goedeke J, Haeberle B, Schmid I, et al. (2011) AFP negative cystic liver lesion in a child should let one think of hepatoblastoma. J Pediatr Hematol Oncol 33:e245–e247. doi:10.1097/MPH.0b013e3181f466ec
85. Meyers RL, Rowland JR, Krailo M, et al. (2009) Predictive power of pretreatment prognostic factors in children with hepatoblastoma: a report from the Children's Oncology Group. Pediatr Blood Cancer 53:1016–1022. doi:10.1002/pbc.22088
86. Ishak KG, Glunz PR (1967) Hepatoblastoma and hepatocarcinoma in infancy and childhood. Report of 47 cases. Cancer 20:396–422. doi:10.1002/1097-0142(1967)20:3<396::AIDCNCR2820200308>3.0.CO;2-O
87. Jha P, Chawla SC, Tavri S, et al. (2009) Pediatric liver tumors–a pictorial review. Eur Radiol 19:209–219. doi:10.1007/s00330-008-1106-7
88. Roebuck DJ, Olsen O, Pariente D (2006) Radiological staging in children with hepatoblastoma. Pediatr Radiol 36:176–182. doi:10.1007/s00247-005-0029-6
89. Czauderna P, Otte JB, Roebuck DJ, et al. (2006) Surgical treatment of hepatoblastoma in children. Pediatr Radiol 36:187–191. doi:10.1007/s00247-005-0067-0
90. Pham TH, Iqbal CW, Grams JM, et al. (2007) Outcomes of primary liver cancer in children: an appraisal of experience. J Pediatr Surg 42:834–839. doi:10.1016/j.jpedsurg.2006.12.065
91. Sasaki F, Matsunaga T, Iwafuchi M, et al. (2002) Outcome of hepatoblastoma treated with the JPLT-1 (Japanese Study Group for Pediatric Liver Tumor) Protocol-1: a report from the Japanese Study Group for Pediatric Liver Tumor. J Pediatr Surg 37:851–856. doi:10.1053/jpsu.2002.32886
92. Faraj W, Dar F, Marangoni G, et al. (2008) Liver transplantation for hepatoblastoma. Liver Transpl 14:1614–1619. doi:10.1002/lt.21586
93. Li JP, Chu JP, Yang JY, et al. (2008) Preoperative transcatheter selective arterial chemoembolization in treatment of unresectable hepatoblastoma in infants and children. Cardiovasc Intervent Radiol 31:1117–1123. doi:10.1007/s00270-008-9373-x
94. Ye J, Shu Q, Li M, et al. (2008) Percutaneous radiofrequency ablation for treatment of hepatoblastoma recurrence. Pediatr Radiol 38:1021–1023. doi:10.1007/s00247-008-0911-0
95. Kulke MH, Mayer RJ (1999) Carcinoid tumors. N Engl J Med 340:858–868
96. Dejong CHC, Parks RW, Currie E, et al. (2002) Treatment of hepatic metastases of neuroendocrine malignancies: a 10-year experience. J R Coll Surg Edinb 47:495–499
97. Sippel RS, Chen H (2006) Carcinoid tumors. Surg Oncol Clin N Am 15:463–478. doi:10.1016/j.soc.2006.05.002
98. Modlin IM, Lye KD, Kidd M (2003) A 5-decade analysis of 13,715 carcinoid tumors. Cancer 97:934–959. doi:10.1002/cncr.11105
99. Soga J (2002) Primary hepatic endocrinomas (carcinoids and variant neoplasms). A statistical evaluation of 126 reported cases. J Exp Clin Cancer Res 21:457–468
100. Takayasu K, Muramatsu Y, Sakamoto M, et al. (1992) Findings in primary hepatic carcinoid tumor: US, CT, MRI, and angiography. J Comput Assist Tomogr 16:99–102
101. Shih WJ, Samayoa L, Shih GL, et al. (2005) Primary hepatic carcinoid tumor presenting as a large multicystic lesion of the liver and on Tc-99 m RBC abdominal imaging showing photopenic areas. Clin Nucl Med 30:530–531. doi:10.1097/01.rlu.0000167507.77894.a7
102. Ulusan S, Kizilkilic O, Yildirim T, et al. (2005) Primary hepatic carcinoid tumor: dynamic CT findings. Abdom Imaging 30:281–285. doi:10.1007/s00261-004-0241-0
103. Komatsuda T, Ishida H, Furukawa K, et al. (2005) Primary carcinoid tumor of the liver: report of a case with an emphasis on contrast-enhanced ultrasonographic findings. J Clin Ultrasound 33:302–304. doi:10.1002/jcu.20132
104. Hirata M, Ishida H, Konno K, et al. (2002) Primary carcinoid tumor of the liver: report of two cases with an emphasis on US findings. Abdom Imaging 27:325–328. doi:10.1107/s00261-001-0069-9
105. Fujino K, Koito K, Sano S, et al. (1998) A primary hepatic carcinoid tumor: evaluation by computed tomography and magnetic resonance imaging. Radiat Med 16:371–373
106. McCarthy SM, Stark DD, Moss AA, et al. (1984) Computed tomography of malignant carcinoid disease. J Comput Assist Tomogr 8:846–850

107. Paulson EK, McDermott VG, Keogan MT, et al. (1998) Carcinoid metastases to the liver: role of triple-phase helical CT. Radiology 206:143–150
108. Maton PN, Miller DL, Doppman JL, et al. (1987) Role of selective angiography in the management of patients with Zollinger-Ellison syndrome. Gastroenterology 92:913–918
109. Bader TR, Semelka RC, Chiu VC, et al. (2001) MRI of carcinoid tumors: spectrum of appearances in the gastrointestinal tract and liver. J Magn Reson Imaging 14:261–269. doi:10.1002/jmri.1182
110. Kuker RA, Mesoloras G, Gulec SA (2007) Optimization of FDG–PET/CT imaging protocol for evaluation of patients with primary and metastatic liver disease. Int Semin Surg Oncol 4:17. doi:10.1186/1477-7800-4-17
111. Virani MJ, Jain S (2002) Primary intraspinal primitive neuroectodermal tumor (PNET): a rare occurrence. Neurol India 50:75–80112
112. Hart MN, Earle KM (1973) Primitive neuroectodermal tumors of the brain in children. Cancer 32:890–897
113. Shah N, Roychoudhury A, Sarkar C (1995) Primitive neuroectodermal tumor of maxilla in an adult. Oral Surg Oral Med Oral Pathol Oral Radiol Endod 80:683–686
114. Charney DA, Charney JM, Ghali VS, et al. (1996) Primitive neuroectodermal tumor of the myocardium: a case report, review of the literature, immunohistochemical, and ultrastructural study. Hum Pathol 27:1365–1369
115. Dehner LP (1986) Peripheral and central primitive neuroectodermal tumors. A nosologic concept seeking a consensus. Arch Pathol Lab Med 110:997–1005
116. Hyun CB, Lee YR, Bemiller TA (2002) Metastatic peripheral primitive neuroectodermal tumor (PNET) masquerading as liver abscess: a case report of liver metastasis in orbital PNET. J Clin Gastroenterol 35:93–97
117. Chang CH, Ramirez N, Sakr WA (1989) Primitive neuroectodermal tumor of the brain associated with malignant rhabdoid tumor of the liver: a histologic, immunohistochemical, and electron microscopic study. Pediatr Pathol 9:307–319
118. Mani S, Dutta D, De BK (2010) Primitive neuroectodermal tumor of the liver: a case report. Jpn J Clin Oncol 40:258–262. doi:10.1093/jjco/hyp158
119. Nair N, Goyal V, Nair CN (1998) Uptake of Tc-99 m MDP by a primitive neuroectodermal tumor of the liver. Clin Nucl Med 23:548–549
120. Sallustio G, Pirronti T, Lasorella A, et al. (1998) Diagnostic imaging of primitive neuroectodermal tumour of the chest wall (Askin tumour). Pediatr Radiol 28:697–702. doi:10.1007/s002470050443
121. Dick EA, McHugh K, Kimber C, et al. (2001) Imaging of non-central nervous system primitive neuroectodermal tumours: diagnostic features and correlation with outcome. Clin Radiol 56:206–215
122. Sabate JM, Franquet T, Parellada JA, et al. (1994) Malignant neuroectodermal tumour of the chest wall (Askin tumour): CT and MR findings in eight patients. Clin Radiol 49:634–638
123. Zhang WD, Chen YF, Li CX, et al. (2011) Computed tomography and magnetic resonance imaging findings of peripheral primitive neuroectodermal tumors of the head and neck. Eur J Radiol 80:607–611. doi:10.1016/j.ejrad.2011.02.008
124. Hari S, Jain TP, Thulkar S, et al. (2008) Imaging features of peripheral primitive neuroectodermal tumours. Br J Radiol 81:975–983. doi:10.1259/bjr/30073320
125. Mani S, Dutta D, De BK (2011) Rare Primitive Neuroectodermal Tumor (PNET) of Liver in a Young Woman. Gastrointest Cancer Res 4:111–113
126. Singh AD, Husson M, Shields CL, et al. (1994) Primitive neuroectodermal tumor of the orbit. Arch Ophthalmol 112:217–221
127. Kiratli H, Bilgic S, Gedikoglu G, et al. (1999) Primitive neuroectodermal tumor of the orbit in an adult. A case report and literature review. Ophthalmology 106:98–102. doi:10.1016/S0161-6420(99)90020-9
128. Yao JC, Pavel M, Phan AT, et al. (2011) Chromogranin A and Neuron-Specific Enolase as Prognostic Markers in Patients with Advanced pNET Treated with Everolimus. J Clin Endocrinol Metab . doi:10.1210/jc.2011-0666
129. Jones JE, McGill T (1995) Peripheral primitive neuroectodermal tumors of the head and neck. Arch Otolaryngol Head Neck Surg 121:1392–1395
130. Jurgens H, Bier V, Harms D, et al. (1988) Malignant peripheral neuroectodermal tumors. A retrospective analysis of 42 patients. Cancer 61:349–357. doi:10.1002/1097-0142(19880115)61:2<349::AIDCNCR2820610226>3.0.CO;2-0